Shock and Vibration 12 (2005) 197–216
IOS Press

An experimental assessment of transverse adaptive fir filters as applied to vibrating structures identification

Daniel A. Castello and Fernando A. Rochinha*
Solid Mechanics Laboratory, Mechanical Engineering Department, COPPE/Federal University of Rio the Janeiro, P.O. Box 68503 – 21945-970 – Rio de Janeiro, RJ, Brasil

Received 13 April 2004
Revised 12 July 2004

Abstract. The present work is aimed at assessing the performance of adaptive Finite Impulse Response (FIR) filters on the identification of vibrating structures. Four adaptive algorithms were used: Least Mean Squares (LMS), Normalized Least Mean Squares ($NLMS$), Transform-Domain Least Mean Squares ($TD-LMS$) and Set-Membership Binormalized Data-Reusing LMS Algorithm ($SM-BNDRLMS$). The capability of these filters to perform the identification of vibrating structures is shown on real experiments. The first experiment consists of an aluminum cantilever beam containing piezoelectric sensors and actuators and the second one is a steel pinned-pinned beam instrumented with accelerometers and an electromechanical shaker.

1. Introduction

In the last years, System Identification [14] has emerged as an important discipline providing valuable tools within the Structural Dynamics Field. The applications are very diverse, ranging from active control of vibrations [25] to model updating [22], passing through damage detection [8] and [13]. Identification is intended to improve the robustness and performance of the involved systems by helping on building reliable models which provide the ground of modern engineering. Those models are used to understand, to control involved phenomena and, probably their key feature, to predict future behavior.

Broadly speaking, identification consists on the process of developing a mathematical model for a real system by combining physical principles with experimental or field data. Therefore, identification uses a priori information, characterized by the model structure and characteristics, and a posteriori data, such as input-output observations. The main idea is to identify a set of parameters such that, over a desired range of operating conditions, the model outputs are close, in some well-defined sense, to the system outputs when both are submitted to the same inputs. Due to the incompleteness of available information and unavoidable measurement errors, system identification only achieves an approximation of the actual system. Usually this mismatch is treated in a task-oriented perspective, meaning that the assessment of an identification performance approach is carried out directly involving the aimed applications [3]. That strongly motivates the development of the present article. It deals with using adaptive Finite Impulse Response (FIR) filter theory [12,23] and [28] to identify second order structural vibrating systems [9] and [25]. Structural dynamics deals, essentially, with three categories of identification, namely: modal parameter identification, model-based parameter identification and control-oriented identification. The first one, often referred to as modal testing, consists on obtaining modal parameters (e.g. damping, mode shapes, frequencies and modal

*Corresponding author. E-mail: faro@serv.com.ufrj.br.

ISSN 1070-9622/05/$17.00

participation factors) that, commonly, are taken as a basis to update analytical models or detect flaws in structures. The second category normally relies on a set of partial differential equations that expresses the physical principles that support the system's response. The sought parameters are physically meaningful and their identification leads to both a reliable modelling and to a deeper understanding of the physics behind the processes. The last approach, which is tailored to control and fault diagnosis applications, often uses the so called black-box models, whose parameters are, normally, physically meaningless. The structure of the model is chosen from established families of finitely parameterised time-domain representations, like, for instance, difference equations. A remarkable feature of those methods is their ability of handling stochastic environments. Indeed, a fourth category, sometimes referred to as grey or semi-physical modelling, must be mentioned. It combines physical insights with parametric representations, like those mentioned above in the last category. It might be interpreted as an intensive use of a priori information in a black-box approach. The capabilities and limitations of a myriad of identification methods included in each one of the aforementioned categories are investigated and reported in a vast literature [1,9,14–16,18,19,21,26] and [11] to cite a few. In the authors opinion, none of them alone can achieve all the goals defined in different applications. Therefore, there is a need of clearly understanding the performance of a determined method when applied to a specific class of problems. That gives rise to the present work, in which the use of FIR filters for modelling structural dynamic systems is assessed by means of a number of experiments.

The remainder of the paper is organized as follows. Section 2 contains general aspects of applying FIR filters to vibrating structures. Section 3 presents the numerical algorithms applied to the parameters identification. Section 4 deals with some illustrative examples to assess the main characteristics of FIR filters modelling in real structures. Finally, Section 5 presents final remarks, comments and future perspectives.

2. Fir filter modelling of vibrating structures

The autoregressive with exogenous excitation (ARX) [21] is a parametric black-box time domain model that describes the system response at a time step n as a function of its response history, system output $\{y(0), y(1), \ldots, y(n-1)\}$, and of the excitation contents, system input $\{u(0), u(1), \ldots, u(n)\}$, viz.

$$y(n) = \sum_{j=0}^{I} a_j u(n-j) + \sum_{k=1}^{K} b_k y(n-k) \tag{1}$$

where $\{b_1, b_2, \ldots, b_K\}$ are the constants known as the autoregressive (AR) parameters and $\{a_0, a_1, \ldots, a_I\}$ are constants constituting the exogenous part of the model. Here, all parameters are supposed to be obtained by means of identification techniques. Once specified the model structure, its order (parsimony), the number of parameters ($I + K + 1$) which, in the context of vibrating structures is connected to the number of degrees of freedom, still remains to be determined.

FIR filters are widely used in signal processing for modelling dynamical systems. They can be interpreted as a particular ARX model in which linear system output at a time step n only depends on the input sequence excitation $\{u(0), u(1), \ldots, u(n)\}$. Thus, they are obtained setting $b_k = 0$ in Eq. (1), viz.

$$y(n) = \sum_{j=0}^{I} a_j u(n-j) \tag{2}$$

and in the Z-domain Eq. (2) casts as

$$\frac{\hat{y}(z)}{\hat{u}(z)} = H(z) = \sum_{j=0}^{I} a_j z^{-j} \tag{3}$$

where $\hat{r}$ denotes the z-transform of a signal r and $H(z)$ is the z-transfer function of the system.

According to Eq. (3), FIR filters do not possess poles. One should notice that despite the fact that FIR filters, at least in principle, are not capable of reproducing resonance behavior so easily [28], they will be used to describe mechanical systems, which possess resonances as an inherent feature. This is partially motivated by the successful

use of FIR filters in mechanical applications like active noise control. In that case, the filters are used to provide models to be used in an adaptive control scheme [28].

The link between vibrating structures and FIR filters can be better understood by investigating the impulse response function of the former. By applying standard techniques, like the Finite Element Method, for the discretization of the continuous equations that govern the dynamics of structural systems, the following second order differential system is achieved

$$\mathbf{M}\ddot{\mathbf{w}} + \mathbf{D}\dot{\mathbf{w}} + \mathbf{K}\mathbf{w} = \mathbf{f} \tag{4}$$

where **M**, **D** and **K** are, respectively, the mass, damping and stiffness matrices and **w** and **f** are displacement and force vectors. Now (4) is rearranged as a first order system by introducing the state vector $\mathbf{x} = [\mathbf{w}^T \quad \dot{\mathbf{w}}^T]^T$ leading to

$$\dot{\mathbf{x}} = \mathbf{A}\mathbf{x} + \mathbf{B}\mathbf{u} \tag{5}$$

$$\mathbf{y} = \mathbf{C}\mathbf{x} \tag{6}$$

where

$$\mathbf{A} = \begin{bmatrix} \mathbf{0} & \mathbf{I} \\ -\mathbf{M}^{-1}\mathbf{K} & -\mathbf{M}^{-1}\mathbf{D} \end{bmatrix} \quad \text{and} \quad \mathbf{B} = \begin{bmatrix} \mathbf{0} \\ \mathbf{M}^{-1}\mathbf{f} \end{bmatrix}$$

and **C** is the output influence matrix which maps the state vector into the observed variables.

The analytical solution of (5) in the time interval $(0, t)$ is formally expressed as

$$\mathbf{x}(t) = e^{\mathbf{A}t}\mathbf{x}(0) + \int_0^t e^{\mathbf{A}(t-\tau)}\mathbf{B}\mathbf{u}(\tau)d\tau \tag{7}$$

Now, considering a division of the time interval into n equally spaced sub-intervals of size Δt and the input $\mathbf{u}(\tau)$ constant in each of those sub-intervals, the following discrete form of (7) is obtained

$$\mathbf{x}(k+1) = \bar{A}\mathbf{x}(k) + \bar{\mathbf{B}}\mathbf{u}(k) \quad k = 0, 1, 2, \ldots \tag{8}$$

with

$$\bar{\mathbf{A}} = e^{\mathbf{A}\Delta t} \qquad \bar{\mathbf{B}} = \int_0^{\Delta t} e^{\mathbf{A}\tau}\mathbf{B}d\tau \tag{9}$$

A slight abuse of notation was adopted in which the argument k stands for $k\Delta t$.

Considering zero initial condition ($\mathbf{x}(0) = \mathbf{0}$), the output $\mathbf{y}(k)$ is obtained from the equation (5) in terms of the previous inputs $\{\mathbf{u}(k-1), \mathbf{u}(k-2), \ldots\}$ as

$$\mathbf{y}(k) = \sum_{i=1}^{k} \mathbf{C}\bar{\mathbf{A}}^{i-1}\bar{\mathbf{B}}\,\mathbf{u}(k-i) = \sum_{i=1}^{k} \mathbf{Y}_i\,\mathbf{u}(k-i) \tag{10}$$

where the matrices $\mathbf{Y}_i = \mathbf{C}\mathbf{A}^{i-1}\mathbf{B}$ above are known as Markov parameters. Actual structural systems are in general damped which implies that some of those parameters almost vanish and therefore the above series may be truncated after a certain number of time steps. Indeed, (10) defines a discrete version of system's impulse response, for more details see [14].

Comparing Eqs (2) and (10) enables the interpretation of the filter coefficients as defining the impulse response of the system by representing the Markov parameters. This establishes a connection between FIR filters and vibrating structures, providing some ground to the identification applications carried out in the present work.

2.1. Adaptive filters

According to Clark [25], an adaptive filter is a self-designing filter that depends upon a recursive algorithm and is capable of performing its duty in the presence of slowly time-varying parameters, where the term slowly refers to the adaptation process. It is well known that, basically, any filter structure can be adapted, i.e., one can construct an adaptive FIR filter, an adaptive infinite impulse response (IIR) filter or an adaptive lattice filter. However, it must be emphasized that since the filter is changing as the system evolves, it is necessary to assure the filter stability at every time step of the process [25]. From this point of view, FIR filters can be considered really compelling inasmuch as their z-transfer function does not possess poles, but only zeros, what is clearly indicated in Eq. (3). Moreover, this type of filter can be easily implemented along with various adaptive algorithms, such as the least-mean-squares (LMS) algorithm. Adaptive FIR filters are well documented in literature [4,23,27], and [5]. Here it is important to emphasize that, generally, more parsimonious identified models are obtained using different ARX filters such as the IIR filter. Such a filter possess not only zeros, but also, poles, what easily enables the reproduction of the actual system dynamics, which leads to lower-order identified filters when compared to using FIR. Nevertheless, the ARX filters are not unconditionally stable, i.e., it is necessary to monitor its stability at every step of the updating process [23,25,28], . Moreover, IIR adaptive algorithms are more complex and computationally intensive presenting slow convergence rates when compared with that of FIR filters.

In order to develop an optimal filter design, one must select a suitable cost function to be minimized. Assuming that the system input and the desired response are zero-mean stochastic processes with wide-sense stationarity, one usually chooses the mean-square value of the error [25] as this cost function. Such quadratic cost function is very attractive since a unique minimum can be assured. The mean square error ξ is defined as follows

$$\xi = \mathcal{E}\ [e^2(n)] \tag{11}$$

where $\mathcal{E}$ stands for the expected value and the error function $e(n)$ for the $n-th$ time step casts as

$$e(n) = d(n) - y(n) \tag{12}$$

where $d(n)$ corresponds to the desired response of the system.

The optimal filter coefficients vector $\mathbf{a}_0$ that minimizes the objective function (11) can be evaluated as follows [23]:

$$\mathbf{R}\,\mathbf{a}_0 = \mathbf{p} \tag{13}$$

where $\mathbf{R}$ and $\mathbf{p}$ are the input signal correlation matrix and the cross-correlation vector between the desired and the input signals respectively, viz.

$$\mathbf{R} = \varepsilon[\mathbf{u}(n)\,\mathbf{u}^T(n)] \tag{14}$$

$$\mathbf{p} = \varepsilon[d(n)\,\mathbf{u}(n)] \tag{15}$$

where the vector $\mathbf{u}(n)$ is

$$\mathbf{u}(n) = \{u(n), u(n-1), \ldots, u(n-I+1)\}^T \tag{16}$$

Such solution is called the Wiener optimal filter. Unfortunately, due to practical limitations, accurate estimates of $\mathbf{R}$ and $\mathbf{p}$ are rarely available.

3. Algorithms

As the following algorithms can be easily found in literature, this section is devoted to present their basic steps and characteristics.

3.1. LMS algorithm

Basically, the LMS algorithms casts as

$$\mathbf{a}(n+1) = \mathbf{a}(n) + \mu\, e(n)\mathbf{u}(n) \tag{17}$$

where μ is the convergence factor of the algorithm and $\mathbf{a}(n)$ is the filter coefficient vector at step n. In order to assure convergence of the coefficients in the mean to optimal solution $\mathbf{a}_0$, the convergence factor μ must be chosen in the range [23]

$$0 < \mu < \frac{2}{\lambda_{\max}} \tag{18}$$

where $\lambda_{\max}$ corresponds to the maximum eigenvalue of the matrix $\mathbf{R}$ [23]. In practice, one may use the following relation [23]

$$0 < \mu < \frac{2}{\mathrm{Tr}(\mathbf{R})} \tag{19}$$

where $\mathrm{Tr}(\mathbf{R})$ denotes the trace of the matrix $\mathbf{R}$. It is significative to obtain an upper bound to the convergence factor μ, nevertheless, it should be remarked that inequality (19) was derived assuming several hypotheses, which are not easily reproduced in engineering applications. Therefore, in most of the cases, the value of μ should not be chosen close to its upper bound [23].

3.2. NLMS algorithm

In order to increase the convergence speed of the LMS algorithm without using estimates of the input signal correlation matrix, a variable convergence factor is a natural solution [23]. Usually, convergence using the Normalized Least-Mean Squares (NLMS) algorithm is easily attained when compared to the LMS case as the choice of the involved parameters is simpler, what might lead to improved convergence rates. For the sake of simplicity, the summary of the adaptation process of the filter coefficients reads as

$$\mathbf{a}(n+1) = \mathbf{a}(n) + \frac{\mu_n}{\gamma + \mathbf{u}^T(n)\mathbf{u}(n)}\, e(n)\mathbf{u}(n) \tag{20}$$

where μ_n is the constant convergence factor and γ is a small constant introduced in the updating formula aiming at avoiding large step sizes when $\mathbf{u}^T(n)\mathbf{u}(n)$ gets very small. The constant convergence factor μ_n must reside in the interval $(0, 2)$. For further details about $NLMS$ algorithm see [23] and [12].

3.3. Transform-domain LMS algorithm

In general it can be shown [6] that for stationary input and sufficiently small convergence factor μ, the speed of convergence of the algorithm is dependent on the eigenvalue spread of the matrix $\mathbf{R}$, i.e., depends on the ratio

$$\frac{\lambda_{\max}}{\lambda_{\min}} \tag{21}$$

where $\lambda_{\max}$ and $\lambda_{\min}$ are the maximum and the minimum eigenvalues of $\mathbf{R}$. Slow convergence rate is expected when ratio (21) is large. When the input signal is highly correlated, one may use the transform-domain algorithm to increase the convergence speed of the LMS algorithm [23,29] and [10]. The basic idea is to somehow transform the input signal $\mathbf{u}(n)$ into another signal with the corresponding autocorrelation matrix having smaller eigenvalue spread. Aiming at this purpose, one may transform the input vector $\mathbf{u}(n)$ in a more convenient vector $\mathbf{s}(n)$, through the application of an orthonormal (or unitary) transform $\mathbf{T}$ [23], viz.

$$\mathbf{s}(n) = \mathbf{T}\mathbf{u}(n) \quad \text{where} \qquad \mathbf{T}\mathbf{T}^T = \mathbf{I}_d \tag{22}$$

where $\mathbf{I}_d$ stands for the identity operator.

Hence the filter output is obtained by multiplying the input $\mathbf{s}$ by the transform-domain filter coefficient vector $\hat{\mathbf{a}}$

$$y(n) = \hat{\mathbf{a}}^T(n)\mathbf{s}(n) \tag{23}$$

The transform-domain filter coefficient update is given as follows

$$\hat{a}_i(n+1) = \hat{a}_i(n) + \frac{2\mu}{\gamma + \sigma_i^2(n)}\, e(n)s_i(n) \tag{24}$$

In Eq. (24) the signals $s_i(n)$ are normalized by their power denoted by $\sigma_i^2(n)$ only when applied in the updating formula such that

$$\sigma_i^2(n) = \alpha\, s_i^2(n) + (1-\alpha)\,\sigma_i^2(n-1) \tag{25}$$

where α is a small factor within the interval $0 < \alpha \leqslant 0.1$ and γ is also a small constant to avoid that the second term of the update equation becomes too large when $\sigma_i^2(n)$ is small.

In matrix form the updating equation casts as follows

$$\hat{\mathbf{a}}(n+1) = \hat{\mathbf{a}}(n) + 2\mu\, e(n)\sigma^{-2}(n)\mathbf{s}(n) \tag{26}$$

where $\sigma^{-2}(n)$ is a diagonal matrix which contains the inverse of the power estimates of the elements $\mathbf{s}(n)$ added to γ [23]. The convergence of the coefficient vector is determined by the eigenvalue spread of $\sigma^{-2}(n)\,\mathbf{R}_s$, where $\mathbf{R_s} = \mathbf{T}\,\mathbf{R}\,\mathbf{T^T}$ [23].

It can be shown that the effect of applying the transformation matrix $\mathbf{T}$ is to rotate the axis such that they become aligned with the principal axis of the hyperellipsoidal equal-error-contours. It should be emphasized that the eccentricity of the error surface remains unchanged by the application of the transformation and so does the eigenvalue spread. Therefore, aiming at reducing the eigenvalue spread, each element of the transform output $\mathbf{s}$ is power normalized, in the updating process, as we can be noticed in equation (24) [23] and [10]. An important topic here is which orthogonal transformation should be used, and this issue is stressed elsewhere in [23,29] and [10]. For the present work, as the signals processed are real, the authors have chosen to use the discrete cosine transform DCT motivated by the experiences reported in [23]. Another approach that can be used to improve the performance of the LMS algorithm is based on the concept of structural subband decomposition [2], what is a generalization of the transform domain adaptive filtering. Doğançay [17] analyses the computational complexity and convergence performance of transform-domain adaptive filtering algorithms including the so-called selective-partial-update strategy for transform-domain algorithms, where the adaptive filter coefficients are segmented into blocks and only a number of these blocks are selected to be updated at every iteration.

3.4. Set-membership binormalized data-reusing LMS algorithm-II

Aiming at speeding up the convergence of the algorithm at the expense of low additional complexity, Diniz and Werner presented the Set-Membership Binormalized Data-Reusing LMS Algorithms [24]. The algorithm requires the introduction of a constraint set H_n which contains all filter coefficient vectors $\mathbf{a}$ that generate an output error $e(n)$ bounded in magnitude by an a priori defined quantity β, viz.

$$H_n = \{\mathbf{a} \in \mathbf{R}^{1+I} / \; |d(n) - \mathbf{a}^T\,\mathbf{u}(n)| \leqslant \beta\} \tag{27}$$

The basic idea consists on designing a filter whose solution belongs not only to H_n, but also to H_{n-1}, i.e.,

$$\mathbf{a}(n+1) \in H_n \cap H_{n-1} \tag{28}$$

Details about the algorithms are presented in [24]. For the present work the authors adopted the Set-Membership Binormalized Data-Reusing LMS Algorithm – II, which will be referred to as $SM-BNDRLMS$ throughout the text. For the sake of simplicity, the summary of the adaptation process of the filter coefficient vector reads as

$$\mathbf{a}(n+1) = \mathbf{a}(n) + \frac{\lambda_1^{'}}{2}\,\mathbf{u}(n) + \frac{\lambda_2^{'}}{2}\,\mathbf{u}(n-1) \tag{29}$$

where

$$\frac{\lambda_1^{'}}{2} = \frac{\eta(n)\, e(n)\, ||\mathbf{u}(n-1)||^2}{||\mathbf{u}(n)||^2\, ||\mathbf{u}(n-1)||^2 - [\mathbf{u}^T(n-1)\,\mathbf{u}(n)]^2} \tag{30}$$

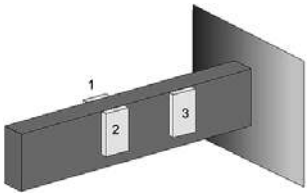

Fig. 1. Flexible beam and its piezoelectric patches – Schematic view.

$$\begin{matrix}\lambda_2^{'} \\ 2\end{matrix} = \frac{\eta(n)\, e(n)\, \mathbf{u}^T(n-1)\, \mathbf{u}(n)}{||\mathbf{u}(n)||^2\, ||\mathbf{u}(n-1)||^2 - [\mathbf{u}^T(n-1)\, \mathbf{u}(n)]^2} \tag{31}$$

$$\eta(n) = \{1 - \beta/|e(n)| \quad \text{if} \quad |e(n)| > \beta; \quad 0 \quad \text{otherwise.}\} \tag{32}$$

Two points should be remarked here, the first one is concerned with the fact that the updating step occurs only if the evaluation of $\eta(n)$ is positive, fact that corresponds to an innovation check as defined by Diniz and Werner [24]. Moreover, in a computational environment where different tasks must be accomplished at the same time, this innovation check reduces the computational burden. The second one is concerned with the denominator of the parameters $\lambda_j^{'}$. Whenever it is zero, the updating of the Set-Membership Normalized LMS ($SM-NLMS$) [24] must be used, which casts as

$$\mathbf{a}(n+1) = \mathbf{a}(n) + \eta(n)\; e(n)\; \frac{\mathbf{u}(n)}{||\mathbf{u}(n)||^2} \tag{33}$$

The computational complexity associated to each one of the aforementioned algorithms is addressed in [12,23] and [24].

4. Illustrative examples

In order to assess the effectiveness of the LMS, the $NLMS$, the $TD-LMS$ and the $SM-BNDRLMS$ algorithms in identifying the coefficients of a FIR filter associated to vibration systems two examples have been explored. The first one consists of an aluminum cantilever beam controlled by means of piezoelectric sensors and actuators and the second one deals with a steel pinned-pinned beam instrumented with accelerometers and excited by an electromechanical shaker.

Before starting the illustrative examples, two issues have to be highlighted at this point. The first one is that the choice of the parameters associated to the identification algorithm was made, as usual, in a heuristic setting by exploring the characteristics of the obtained signals and leaded by theoretical bounds resulting from convergence requirements established in [12,23] and [24]. The second one is that an estimate of the order of the system can be obtained by different techniques, nevertheless, it should be emphasized that most of them demand great computational burden. Therefore, these techniques have not been presented and used inasmuch as they introduce a characteristic that is out of the simplicity embedded in using FIR filters.

4.1. Cantilever beam

The testbed for the first experiment is depicted in Figs 1 and 2, where the piezoelectric patches number 1 and 2 perform as an actuator and the piezoelectric patch number 3 as a sensor. The beam is made of aluminium with an elasticity modulus equal to 71 GPa. The dimensions of the beam are: 500 $\times$ 20 $\times$ 1.5 mm, however its free length is 414 mm. The dimensions of the PZT (lead zirconium titanate) piezoelectric patches are: 25 $\times$ 20 $\times$ 0.5 mm and their elastic modulus is equal to 61 GPa. The relative permittivity ϵ_{31} is 1750 and the piezoelectric constant d_{31} is -125×10^{-12} m/V. More details about the experimental setup can be found in [7] and [20]. Table 1 contains the information concerning the analyzed cases throughout the work.

Table 1
Analyzed cases

Case	Experiment	I+1	LMS	$NLMS$	$TD-LMS$	$SM-BNDRLMS$
$C1$	1	2	$\mu = 0.0005$	$\mu_n = 1$ $\gamma = 0.001$	- -	$\beta = 0.0173$
$C2$	1	10	$\mu = 0.0005$	$\mu_n = 1$ $\gamma = 0.001$	- -	$\beta = 0.0173$
$C3$	2	$]10, 400[$	$\mu \in]0.01, 0.1[$	$\mu_n \in]0.1, 1.9[$ $\gamma = 0.001$	- -	- -
$C4$	2	2	$\mu = 16.67$	- -	$\mu = 16.67$	$\beta = 0.0130$
$C5$	2	2	$\mu = 4.167$	- -	$\mu = 4.167$	- -
$C6$	2	200	$\mu = 1/7$	$\mu_n = 1.0$ $\gamma = 0.001$	$\mu = 1/200$	$\beta = 0.087$

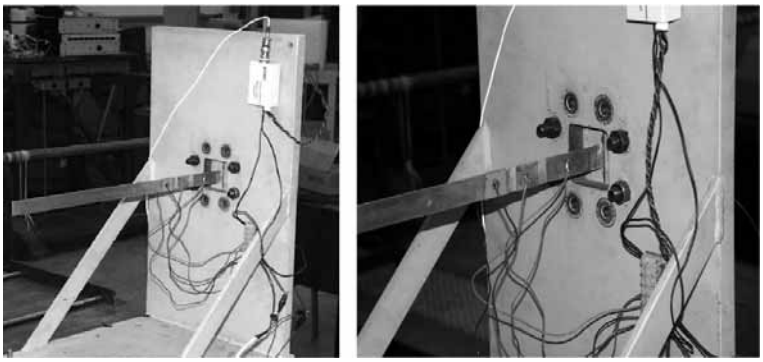

Fig. 2. Experimental setup: general view (left) and zoom on the sensing-actuating system (right).

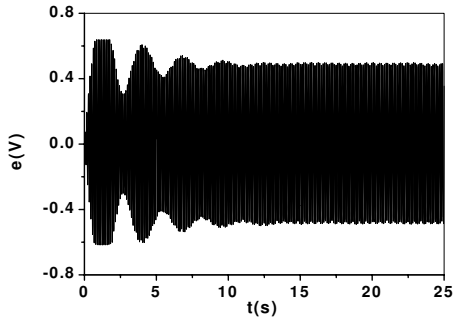

Fig. 3. System response for case $C1$.

4.1.1. Experimental data

In the first case to be analyzed ($C1$), the system input is a sinusoidal signal with frequency equal to 8.9 Hz and amplitude of 10 V. The sampling frequency is 100 Hz and the signals have been recorded from 0 to 25 seconds. The system response, in Volts, is graphed in Fig. 3.

The convergence factor μ was set equal to 0.0005, the $NLMS$'s properties μ_n and γ were set equal to 1 and to 0.001 respectively and the upper bound on the magnitude of the error β is equal to 0.0173. Here, the parameter β was chosen based on the standard deviation of the error of the the $NLMS$ algorithm between the instants $t = 10$ s and $t = 25$ s. A filter with 2 coefficient was adopted. The responses provided by the filters based on the LMS, $NLMS$ and $SM - BNDRLMS$ algorithms will be denoted by y, y_n and y_s respectively and the corresponding error functions by e, e_n and e_s, such that

$$e = d - y \qquad e_n = d - y_n \qquad e_s = d - y_s \tag{34}$$

Figures 4, 5 and 6 depict the error between the desired response d and the filter responses y, y_n and y_s respectively.

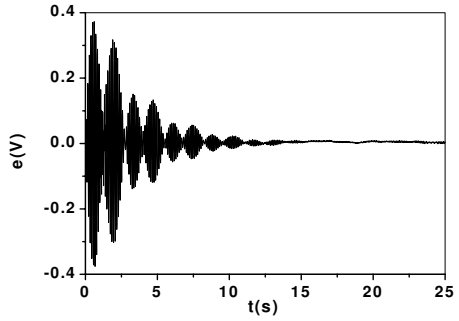

Fig. 4. Error evolution – LMS algorithm applied to case $C1$.

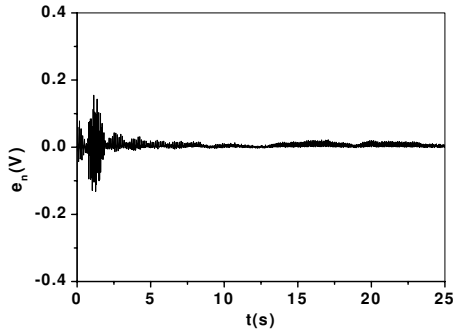

Fig. 5. Error evolution – $NLMS$ algorithm applied to case $C1$.

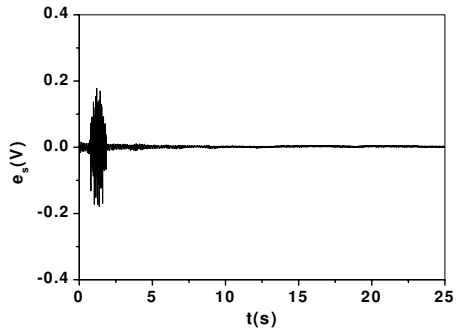

Fig. 6. Error evolution – $SM - BNDRLMS$ algorithm applied to case $C1$.

Figure 4 presents the error of the filter using the LMS algorithm, and there is no doubt that the adaptive system was able to reproduce the system response effectively starting at the instant $t = 15$ s approximately. Figure 5 depicts the error of the filter using the $NLMS$ algorithm, and as one can notice, it also was effective in reproducing the desired response, nevertheless, it took less time than the LMS algorithm. This different behaviour was already expected inasmuch as the $NLMS$ algorithm utilizes a variable convergence factor aiming at minimizing the instantaneous output error. Figure 6 depicts the error of the filter using $SM - BNDRLMS$ algorithm and it presents a behaviour similar to $NLMS$ in the beginning of the period but it is able to decrease the level of error in the response. This characteristic is reported in [24], i.e., the $SM - BNDRLMS$ is capable of obtaining low-excess mean-squared error [23]. Moreover, the number of updates of the $SM - BNDRLMS$ was 1596 while LMS and $NLMS$ had updates at each iteration, i.e., 2500 iterations.

For the second case to be analyzed ($C2$), everything has been maintained equal to case $C1$ but the number of filter coefficients, which were increased from 2 to 10. Figures 7, 8 and 9 depict the error functions for this new adaptive

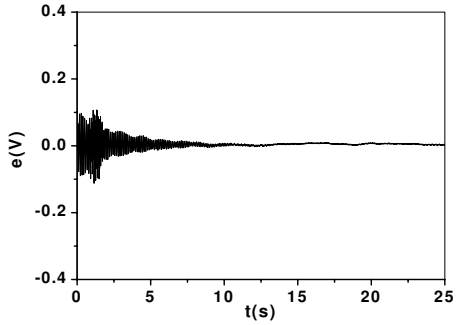

Fig. 7. Error evolution – LMS algorithm applied to case $C2$.

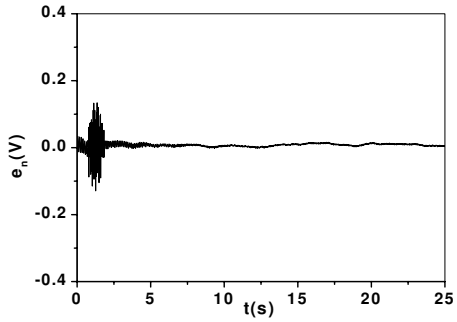

Fig. 8. Error evolution – $NLMS$ algorithm applied to case $C2$.

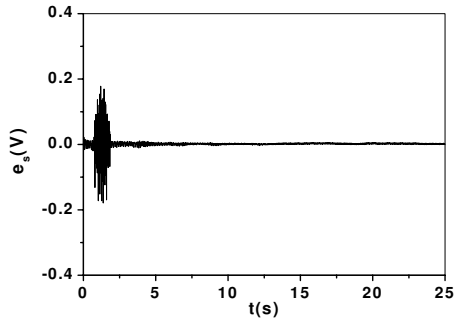

Fig. 9. Error evolution – $SM - BNDRLMS$ algorithm applied to case $C2$.

system corresponding, respectively, to LMS, $NMLS$ and $SM - BNDRLMS$ algorithms. One should notice that the increase in the number of filter coefficients has led to a higher efficiency of the adaptive algorithms LMS and $NLMS$, which, in particular, was remarkable for the LMS algorithm. The H_2 norm of e [30], which expresses the integral of e^2 over the observed period, has decreased from 20.19 to 9.07, whereas the same norm of the error function e_n has decreased slightly from 7.90 to 7.27. Despite the fact that case ($C2$) considered a ten-coefficient filter, it should be emphasized that for an input composed of only one single frequency, a two-coefficient filter is able to identify the system as it was shown for case ($C1$).

4.2. Pinned-pinned beam

The testbed for the second experiment is depicted in Figs (10) and (11). The beam is made of steel and its dimensions are: 1467 $\times$ 76.2 $\times$ 7.9 mm. Four piezoelectric accelerometers: 33B52-PCB-PIEZOTRONICS were used. Starting from the left end of the beam, the accelerometers are located at 1/4, 1/3, 1/2 and 5/6 of the beam

Table 2
Natural frequencies (Hz) for the pinned-pinned beam

Mode no.	Experimental	FEM
1	8.6	8.6
2	33.6	34.4
3	75.8	77.3

Table 3
Experiment setup

Experiment no.	Excitation type	sampling frequency (Hz)	cut-off frequency (Hz)	t_f (s)
1	white-noise	400	100	12.5
2	sine-chirp (0-100) Hz	800	100	8
3	$\sin(68\pi)$	800	100	4
4	$\sin(150\pi)$	800	100	4

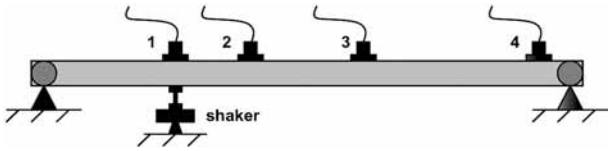

Fig. 10. Testbed sketch of the second experiment.

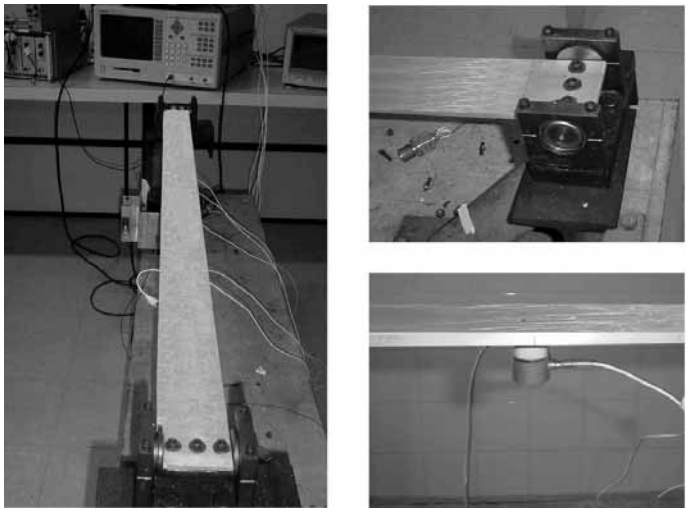

Fig. 11. Experimental setup (second experiment).

length. Although there were four available accelerometers, only the number 1, placed in a collocated disposition, was used for the adaptation processes.

Tables 2 and 3 present the first three natural frequencies obtained both experimentally and by a Finite Element Analysis (FEM). Data acquisition parameters utilized for all experiments are shown as well.

For the sake of clarity, the analysis of some results was based on the following normalized global error indicators:

$$E = \frac{\|e\|}{\|d\|} \times 100\,\% \tag{35}$$

$$E_n = \frac{\|e_n\|}{\|d\|} \times 100\,\% \tag{36}$$

where $\|\ \|$ states for the H_2 norm of time signals.

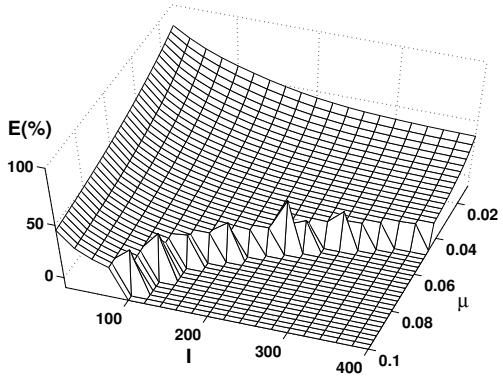

Fig. 12. LMS global errors E of the identified models, case $(C3)$.

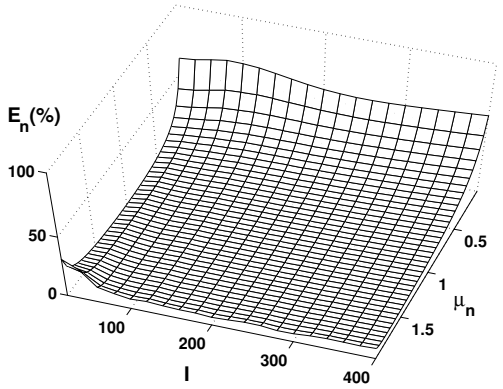

Fig. 13. $NLMS$ global errors E of the identified models, case $(C3)$.

Aiming at assessing the practical influence of filter's parsimony and convergence factors μ and μ_n, for LMS and $NLMS$ algorithms, (case $(C3)$) is analyzed. Case $(C3)$ uses data provided by experiment 2 (see Table 2), in which the structure is excited by a sine-chirp signal.

Figures 12 and 13 depict, in a compact fashion, the global errors E and E_n corresponding to LMS and $NLMS$ algorithms for 800 different cases. Since the adaptation process based on the LMS algorithm has some stability conditions which must be satisfied, given by Eq. (19), it was already expected that for some values of I and μ, convergence would not be reached.The flat region in the graph of Fig. 12 corresponds to the values of I and μ which did not provide the required convergence conditions. The $NLMS$ algorithm provided accurate results as one can see in Fig. 13. Two points should be remarked, the first one concerns the convergence issue, which was not a problem in any of the analyzed adaptation processes. The second is the fact that for $\mu_n \geqslant 1.0$, the accuracy of the adaptation process is approximately the same for 100, 200, 300 or 400 coefficients, for these experimental data.

The next two situations to be analyzed concern the beam identification using the LMS, $TD-LMS$ and $SM-BNDRLMS$ algorithms. The first example, case $(C4)$, considers the experiment number 4 of table (2) and an adaptive filter with two coefficients. For this excitation signal, the experimental input signal correlation matrix $\mathbf{R}$ has an eigenvalue spread of 10.86, its maximum eigenvalue is $\lambda_{\max} = 2.4 \times 10^{-3}$ and the numeric input signal correlation matrix has the same eigenvalue spread of the experimental ones's and a maximum eigenvalue $\lambda_{\max} = 2.9 \times 10^{-3}$. Hence, as a reference an eigenvalue λ equal to 3×10^{-3} was taken. The adaptation processes based on LMS and $TD-LMS$ algorithms consider a convergence factor $\mu = (20\,\lambda)^{-1}$ and the $SM-BNDRLMS$ a bound $\beta = 0.0130$.

Figure 14 shows the experimental desired response and Figs 15, 16 and 17 show the errors of the LMS, $TD-LMS$ and $SM-BNDRLMS$ algorithms. It is clear that the three algorithms effectively achieved to identified models that reproduce the actual response of the system. However, aiming at obtaining a closer look at the parameter

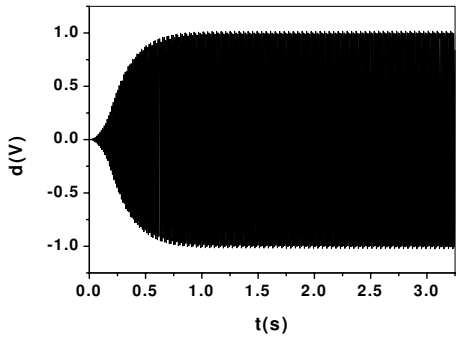

Fig. 14. Desired response for experiment 4.

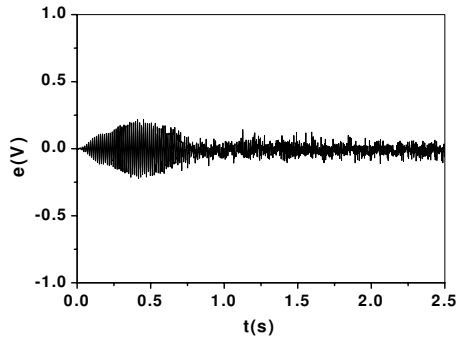

Fig. 15. Error function based on the LMS algorithm for the case $C4$.

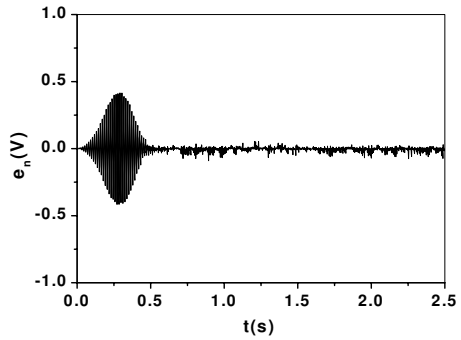

Fig. 16. Error function based on the transform-domain LMS algorithm for the case $C4$.

convergence issue, one may define a normalized filter coefficient ω_j defined as follows

$$\omega_j(n) = \frac{a_j(n)}{a_{o,j}} \tag{37}$$

where $a_j(n)$ and $a_{o,j}$ correspond to the $j-th$ filter coefficient at the $n-th$ iteration and to the $j-th$ component of the optimum solution $\mathbf{a}_o$. Figures 18 and 19 show the evolution of the normalized parameters along the iterations for the LMS and for the transform-domain LMS algorithms.

From Figs 18 and 19 it is clear that the transform-domain accelerated the convergence of the filter coefficients. The LMS algorithm required more than 1500 iterations to achieve convergence while for the transform-domain LMS it was accomplished with at most 1100 iterations. From Fig. 20 it is clear that the second component of the filter coefficient based on the $SM-BNDRLMS$ achieved convergence at iteration number 1000 approximately while the

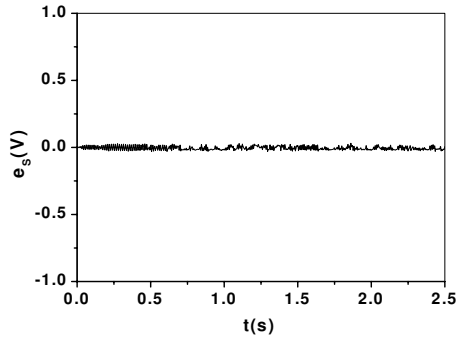

Fig. 17. Error function based on the $SM - BNDRLMS$ algorithm for the case $C4$.

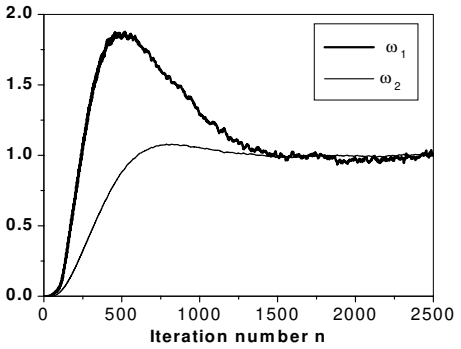

Fig. 18. Evolution of the normalized filter coefficients (LMS), case ($C4$).

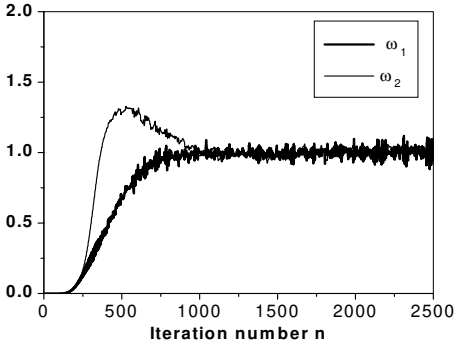

Fig. 19. Evolution of the normalized filter coefficients (transform-domain LMS), case ($C4$).

first component of the filter starts oscillating around the optimum value at iteration number 1000. Nevertheless, the mean value of each filter coefficient is close to its respective optimum value and moreover, the $SM - BNDRLMS$ had only 1093 updates while LMS and $TD - LMS$ had 2500 ones.

As a last comparison of $LMS, TD - LMS$ and $SM - BNDRLMS$ algorithms, case ($C5$), experiment number 3 of Table 2 was considered. The main difference is concerned with the eigenvalue spread of the experimental input signal correlation matrix $\mathbf{R}$, which is equal to 55.2 and its maximum eigenvalue is $\lambda_{\max} = 2.9 \times 10^{-3}$. Therefore, once again the reference eigenvalue $\lambda = 3 \times 10^{-3}$, filter's order $I + 1 = 2$ and the convergence factor $\mu = (80 \times \lambda)^{-1}$. Figures 21, 22 and 23 depict the convergence of the normalized filter coefficients. It should be emphasized that for the present example, the eigenvalue spread is 5 times greater than in the previous one. For the present case both $TD - LMS$ and $SM - BNDRLMS$ algorithms provided an effective identification and the

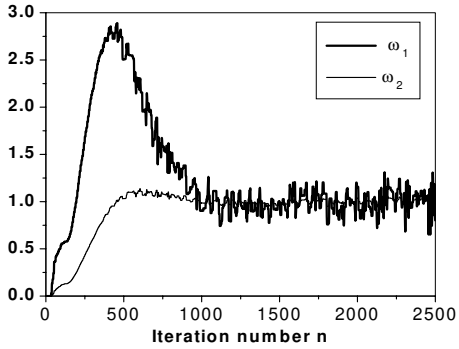

Fig. 20. Evolution of the normalized filter coefficients ($SM - BNDRLMS$), case ($C4$).

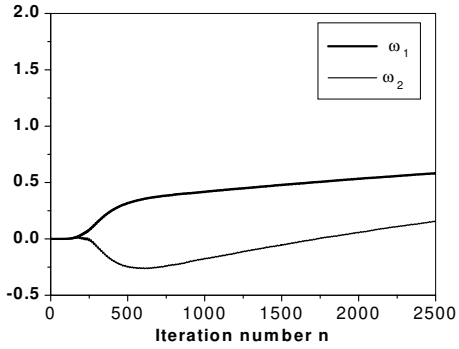

Fig. 21. Evolution of the normalized filter coefficients (LMS), case ($C5$).

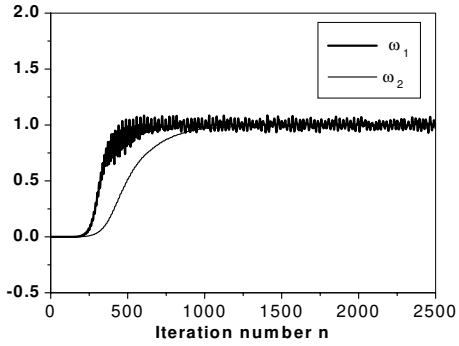

Fig. 22. Evolution of the normalized filter coefficients (transform-domain LMS), case ($C5$).

LMS algorithm could not reach convergence for the available period of time. Here it is worth mentioning that $SM - BNDRLMS$ algorithm only used 1499 updates while LMS and $TD - LMS$ algorithms had 2500 ones.

It is worthwhile to mention that, so far, every performed identification have not dealt, as the applied excitation signals were composed of only one single frequency, with mismodelling issues, which, here, are attributed mainly to the order of the applied filter.

Aiming at investigating an identification process through which a broad-band input signal is used to excite the beam, and in which, mismodelling will probably play a role, case ($C6$) deals with experiment number 1 data. As the input is a white-noise excitation, it is expected that minimizing the error function will force the filter coefficients to approach the impulse response of the system.

Before analyzing the identified models produced by the algorithms presented here, one should give a closer look

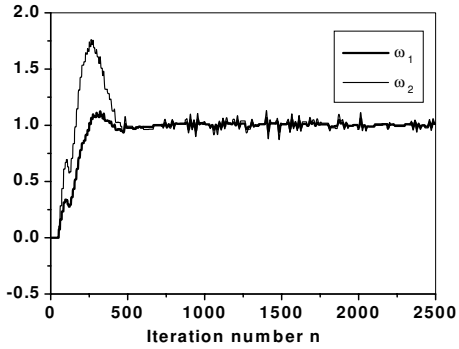

Fig. 23. Evolution of the normalized filter coefficients ($SM - BNDRLMS$), case ($C5$).

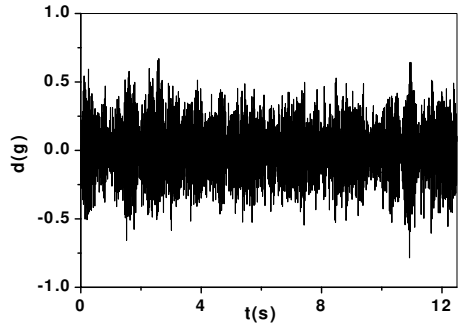

Fig. 24. Response of the first accelerometer for case $C6$.

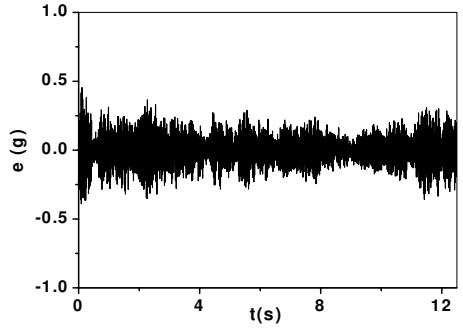

Fig. 25. Error function based on the LMS algorithm for the case $C6$.

at the level of the error signal and to the effect of averaging on the filter coefficient vector. For this purpose, the LMS algorithm is used. At a first step, a filter with 200 coefficients and a convergence factor $\mu = \frac{1}{7}$ was adopted. The response of the accelerometer number one, in g units, is depicted in Fig. 24 and the error provided by the LMS algorithm is presented in Fig. 25.

At this point, it is important to emphasize that, unlike what happened in the previous examples, the ratio between the error e and the output acceleration d implies that the identified model is not acceptable in applications imposing very stringent precision requirements. Indeed, it is exactly what was expected, due to the limitations of the identification process imposed by mismodelling combined with measurement noise. A direct way of improving the quality of the identified models is provided by enlarging the number of used filters, what can be interpreted as an attempt of better approximating the non finite dynamics of the system to be identified. The performance of this strategy that led to an improvement of the identified models is presented in Fig. 26, in which were used 300, 400, 500 and 1000 filter

Table 4
Running time for the algorithms

LMS	$NLMS$	$SM-BNDRLMS$	$TD-LMS$	t_f (s)
2.03 s	2.15 s	2.75 s	376.02 s	12.50 s

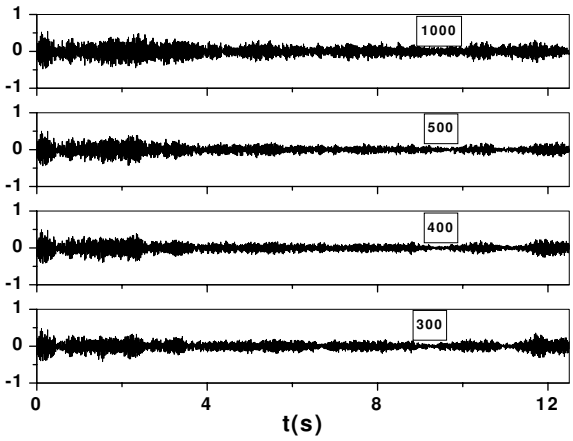

Fig. 26. Error function, in g units, based on the LMS algorithm for case $C6$ for 300, 400, 500 and 1000 filter coefficients.

coefficients.

This very intuitive approach reveals not to be feasible as it presents some significant limitations. The first, and probably the most serious, relies on difficulties of real time implementations due to the computational burden associated to the great number of required numerical operations. The second limitation is linked to the fact that in order to assure convergence, the factor μ must be reduced which in turn implies in a larger period of time to accomplish the identification. The last issue to be mentioned is the capture of high frequency dynamics associated to the noise in measurements.

Another way of improving the LMS, as well as any other algorithm performance, is substitute the updated filter coefficients by an average involving their last values. Figure 27 depicts a comparison, in the frequency domain, between the frequency response function (FRF) of the system directly provided by an frequency analyzer (denoted by EXP) with the system identified by means of the LMS algorithm. In Fig. 27 the symbol ($\bigtriangledown$) is the representation, in the frequency domain, of the last filter coefficient vector $\mathbf{a}(n)$ as the symbol ($\circ$) is the representation of the average of the filter coefficient vector $\mathcal{E}[\mathbf{a}(n)]$. The averaging process started at the instant $t = 9.4$ s, which corresponds, in this case, to $\frac{3}{4}$ of the final instant t_f of the experiment. It is clear from Fig. 27 that the average of the filter coefficient vector provides a more consistent result than the one provided by the last filter coefficient vector. This characteristic of the mean value of the filter coefficient vector is stressed elsewhere [23].

The comparison of the performance of the different algorithms mentioned before is now carried out. A comparison in the frequency domain will be done considering the identified systems by LMS, $NLMS$, $TD-LMS$ and $SM-BNDRLMS$ algorithms and, for each one of them, an average of its respective filter coefficient vector. For this, the following parameters have been chosen: $I+1 = 200$, $\mu = \frac{1}{7}$, $\mu_{TD} = 1/200$ (convergence factor for the $TD-LMS$ algorithm), $\mu_n = 1.0$, $\gamma = 0.001$, $\alpha = 0.025$ and $\beta = 0.087$.

Figure 28 depicts the representation of systems identified by means of the LMS, $NLMS$, $TD-LMS$ and $SM-BNDRLMS$ algorithms, one identified by means of the Eigensystem Realization Algorithm with Data Correlations (ERA/DC) [14] and the direct frequency response function H of the system. The identification by means of the ERA used the response coming from all the available accelerometers shown in Fig. 10 and took into account the experimental information within the band (0,100) Hz and it was added to the comparisons due to the fact that it is a well know identification technique in the vibration and modal analysis community. The data used for the direct frequency response function and for the ERA/DC had a sampling frequency of 400 Hz and cut-off frequency of 100 Hz.

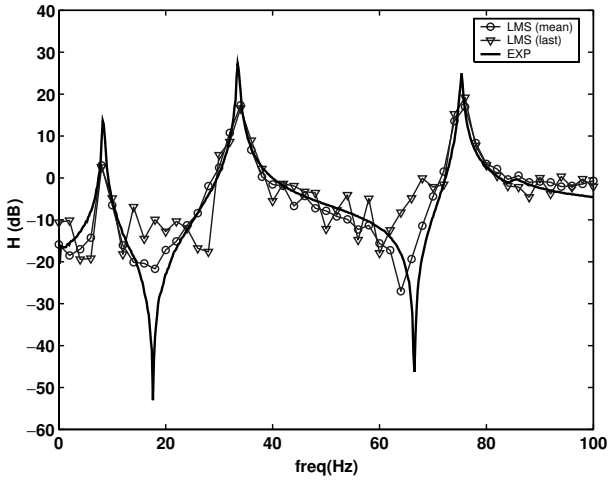

Fig. 27. Frequency-domain representation of the identified system by means of the LMS algorithm for case $C6$ ($\circ$: average of the filter coefficient vector and $\bigtriangledown$: last filter coefficient vector).

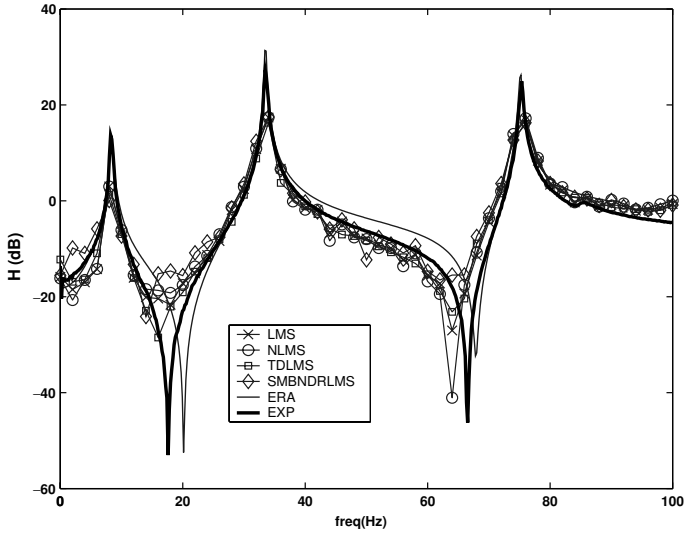

Fig. 28. Identified systems for case $C6$.

It is clear from Fig. 28 that, despite the specific differences, all the LMS-based algorithms were able to capture the essence of the system dynamics, although the anti-resonances were not fully captured. The ERA was also able to capture the essence of the system, although it did not capture the anti-resonances either. A closer look at the system provided by the $SM - BNDRLMS$ reveals some small oscillations, but it has to be highlighted that only 1746 updates were necessary which represents, from the computational standpoint, a gain as all the other algorithms required at least 5000 iterations.

The running time of the algorithms, for an off-line identification, is shown in Table 3. Two points should be remarked here. The first one is associated to the fact that, the final instant of time of the experimental signals is $t_f = 12.5$ s and that the LMS, $NLMS$ and $SM-BNDRLMS$ performed all the required numerical operations in a period less than 3 s, i.e., they would probably accomplish their task in an on-line environment system identification process. Nevertheless, although the $TD - LMS$ algorithm provided an effective identification the period of time required to perform all the numerical operations was 376.02 s, due to the fact that the discrete cosine transformation had to be applied at every iteration of the algorithm.

Some points need to be highlighted now. The first one is that although $TD-LMS$ algorithm is aimed at accelerating the convergence rate of the LMS, the length of the adaptive filter is a more critical issue than it is for LMS, $NLMS$ and $SM-BNDRLMS$ algorithms. Such thing happens due to the required operations involved in the calculation of the unitary transformation of the vectors $\mathbf{u}(n)$. In a situation in which a large number of filter coefficients is required the complexity of the orthogonal transform and power normalization can be reduced by using a selective-partial-update strategy as reported in [17]. The second concerns the input signal and the transformation that was used here, i.e., the DCT was only one possibility among a myriad. Unfortunately, due to the mismodelling problem combined with measurement noise, and to the large number of coefficients, it is difficult to analyze the evolution of each filter coefficient as it was accomplished before.

5. Concluding remarks

In the present work, vibrating systems were successfully identified by FIR filters combined with adaptive algorithms. The effectiveness of the method was assessed on experimental data and the provided results may be considered compelling and effective for the examples that were considered. Such examples have considered different types of excitation such as harmonic, sine-chirp and white-noise. The filter adaptation was performed using four LMS-based algorithms, LMS, $NLMS$, $TD-LMS$ and $SM-BNDRLMS$. A comparison of the models identified by means of FIR filters and ERA with the experimental FRF was carried out. This comparison showed a good agreement between the model identified by means of FIR filters with the direct frequency response function of the system. It should be remarked that the $SM-BNDRLMS$ algorithm seems to be prone to be used in control applications inasmuch as it is able to obtain low-excess mean-squared error and to the fact that it does not need to update its filter coefficients at every iteration, what is very attractive for real time implementation. A point to be emphasized is that this type of identification, at least in principle, does not furnish any relation between the filter coefficients and the physical parameters of the system. Nevertheless, one should remark that this method possesses a relatively simple and stable implementation what enables its use in on-line identification involving situations where fast analysis is required to indicate any system's change that can be considered a signal of damage or faults.

Acknowledgement

The authors are grateful to professor Paulo Sergio Ramirez Diniz from the Electrical Engineering Department of Federal University of Rio de Janeiro for his fruitful considerations about the adaptive algorithms. The authors would like also to express their gratitude to professors Ney Roitman and Carlos Magluta from Civil Engineering Department of Federal University of Rio de Janeiro who provided the experimental framework used in the present article.

References

[1] A. Florakis, S.D. Fassois and F.M. Hemez, MIMO LMS-ARMAX Identification of Vibrating Structures-Part II: A Critical Assessment, *Mechanical Systems and Signal Processing* **15**(4) (2001), 737–758.

[2] A. Mahalanobis, S. Song, S.K. Mitra and M.R. Petraglia, Adaptive FIR Filters Based on Structural Subband Decomposition for System Identification Problems, *IEEE Transactions on Circuits and Systems-II: Analog and Digital Signal Processing* **40**(6) (1993), 375–381.

[3] A.T. Morris, *Comparing Parameter Estimation Techniques for an Eletrical Transformer Oil Temperature Prediction Model*, Nasa/TM – 1999-208974.

[4] B. Widrow, Adaptive Filters, in: *Aspects of Network and Systems Theory*, R.E. Kalman and N. Declaris, eds, New York: Holt, Rinehart and Winston, 1970, pp. 563–587.

[5] B. Widrow, J.R. Glover, J.M. Mccool, J. Kaunitz, C.S. Wiliams, R.H. Hearn, J.R. Zeidler, E. Dong and R.C. Goodlin, Adaptive Noise Cancelling: Principles and Applications, *Proceedings of the IEEE* **63**(12) (1975), 1692–1716.

[6] B. Widrow, J.M. Mccool, M.G. Larimore and C.R. Johnson, Stationary and non Stationary Learning Characteristics of LMS Adaptive Filter, *Proceedings of the IEEE* **64**(8) (1976), 1151–1162.

[7] C.A.O. Martins, Control of Flexible Structures Using Piezoelectric Patches in: *Portuguese*, M.Sc. Thesis, ed., Solid Mechanics Laboratory, UFRJ, Rio de Janeiro, Brasil, 1999.

[8] D.A. Castello, L.T. Stutz and F.A. Rochinha, A Structural Defect Identification Based on a Continuum Damage Model, *Computers & Structures* **80** (2002), 417–436.
[9] D.A. Castello and F.A. Rochinha, *Adaptive Filter Theory Applied on Mechanical System Identification*, Brazilian Congress of Mechanical Engineering, Uberlândia, M.G., Brasil, 2001.
[10] D.F. Marshall, W.K. Jenkins and J.J. Murphy, The Use of Orthogonal Transforms for Improving Performance of Adaptive Filters, *IEEE Transactions on Circuits and Systems* **36**(4) (1989), 474–484.
[11] F.M. Hemez and S.W. Doebling, Review and Assessment of Model Updating for Non-Linear, Transient Dynamics, *Mechanical Systems and Signal Processing* **15**(1) (2001), 45–74.
[12] G.O. Glentis, K. Berberidis and S. Theodoridis, Efficient Least Squares Adaptive Algorithms for FIR Transversal Filtering, *IEEE Signal Processing Magazine*, **16**(4) (1999), 13–41.
[13] H.G. Natke and C. Cempel, *Model-Aided Diagnosis of Mechanical Systems – Fundamentals, Detection, Localization, Assessment*, Springer Verlag, Germany, 1997.
[14] Jer-Nan Juang, *Applied System Identification*, Prentice Hall, New Jersey, USA, 1994.
[15] K.A. Petsounis and S.D. Fassois, Parametric Time-domain Methods for the Identification of Vibrating Structures – A Critical Comparison and Assessment, *Mechanical Systems and Signal Processing* **15**(6) (2001), 1031–1060.
[16] K.A. Woodbury, *Inverse Engineering Handbook*, CRC Press, 2003.
[17] K. Doğançay, Complexity Considerations for Transform-Domain Adaptive Filters, *Signal Processing* **83** (2003), 1177–1192.
[18] K.F. Alvin, L.D. Peterson and K.C. Park, Method for Determining Minimum-order Mass and Stiffness Matrices from Modal Test Data, *AIAA Journal* **33**(1) (1995), 128–135.
[19] K. Ma and J. Melcher, Adaptive Modelling and Eigen-Parameter Identification of Structures Based on the MX Filter and CMX-LMS Algorithm, *Mechanical Systems and Signal Processing* **17**(2) (2003), 345–360.
[20] L.C. Oliveira, Identification and Control: An Application on Flexible Structures using Piezoelectric Materials, in: *Portuguese*, M.Sc. Thesis, ed., Solid Mechanics Laboratory, UFRJ, Rio de Janeiro, Brasil, 2003.
[21] L. Ljung, *System Identification – Theory for the User.*, Prentice Hall, USA, 1987.
[22] M.I. Friswell and J.E. Mottershead, *Finite Element Model Updating in Structural Dynamics* Kluwer, 1995.
[23] P.S.R. DINIZ, *Adaptive Filtering*, Kluwer Academic Publishers, USA, 1997.
[24] P.S.R. Diniz and S. Werner, Set-Membership Binormalized Data-Reusing LMS Algorithms, *IEEE Transactions on Signal Processing* **51**(1) (2003), 124–134.
[25] R.L. Clark, W.R. Saunders and G.P. Gibbs, *Adaptive Structures*, John Wiley and Sons Inc., USA, 1998.
[26] S.D. Fassois, MIMO LMS-ARMAX Identification of Vibrating Structures–Part I: The Method., *Mechanical Systems and Signal Processing* **15**(4) (2001), 723–735.
[27] S.J. Elliot, I.M. Stothers and P.A. Nelson, *A Multiple Error LMS Algorithm and Its Application to the Active Control of Sound and Vibration*, IEEE Transactions on Acoustics, Speech and Signal Processing ASSP-35 (10), 1987, pp. 1423–1434.
[28] S.M. Kuo and D.R. Morgan, *Active Noise Control Systems*. John Wiley and Sons Inc., USA, 1996.
[29] S.S. Narayan, A.M. Peterson and M.J. Narasimha, Transform Domain LMS Algorithm, *IEEE Transactions on Acoustics, Speech, and Signal Processing* **31**(3) (1983), 609–615.
[30] W.K. Gawronski, *Dynamics and Control of Structures: A Modal Approach*, Mechanical Engineering Series, Springer-Verlag, New York, 1998.